Application of Plane Waves for Accurate Measurement of Microwave Scattering from Geophysical Surfaces

Sivaprasad Gogineni, K. C. Jezek, Leon Peters, Jr., *Life Fellow, IEEE*, Jonathan D. Young, *Member, IEEE*, Scott G. Beaven, and E. M. Nassar

***Abstract*—We utilized the concept of a compact antenna range to obtain plane-wave illumination to accurately measure scattering properties of simulated sea ice. We also made simultaneous measurements using conventional antennas.**

Measured scattering coefficients obtained with the plane-wave system at 10 GHz decreased by about 35 dB when the incidence angle increased from 0° to 10°. Scattering coefficients derived from data collected with the radar system at 13.5 GHz using conventional far-field antennas decreased by about 20 dB over the same angular region. This demonstrates that the far-field properties of a widebeam antenna are inadequate for measuring the angular scattering response of smooth surfaces.

We believe that application of the compact antenna range concept for scattering measurements has a wide range of applications and is the solution to the long-standing problem of how to directly measure scattering consisting of coherent and incoherent components.

I. Introduction

APPLICATION of microwave sensors to remote sensing of sea ice is well documented [1]–[7]. Active and passive microwave sensors have been and are being used for operational and scientific monitoring of sea ice [8], [9]. However most of the current data inversion algorithms are qualitative and empirical. To make these algorithms more robust and quantitative, the Office of Naval Research (ONR) initiated a multidisciplinary research program. The goals of this program are to understand better the physics of scattering and emission from various types of sea ice; to develop forward scattering and emissivity models; and to develop inverse scattering models to extract sea ice geophysical parameters from electromagnetic signatures. As a part of this research program, we developed a laboratory technique for accurately measuring the scattering properties of saline ice using plane waves.

Calibrated radar systems, referred to as scatterometers, are used for scattering measurements over distributed targets. These systems generally utilize far-field properties of an antenna. Because scattering from smooth surfaces decays rapidly with incidence angle, either a very narrow antenna beam or some algebraic manipulation is required to extract the true scattering response. But traditional technical solutions require use of a very large aperture antenna, which is impractical in the laboratory environment. Algebraic solutions require *a priori* knowledge of the scattering response. These problems can be solved by the application of the compact antenna range concept to determine directly the scattering response [10].

A compact range uses a large reflector antenna to transform spherical wavefronts from the feed antenna into planar wavefronts. We used an offset reflector antenna to provide plane-wave illumination. With this antenna we collected backscatter data over simulated sea ice at the Cold Regions Research and Engineering Laboratory (CRREL). The ice was grown in an outdoor pit with dimensions of 18 by 8 m. We made these measurements over incidence angles from 0° to 35° with VV polarization at 10 GHz. For comparison, we also made backscatter measurements using a 13.5-GHz system with diagonal horn antennas operated in the far-field. These measurements were also made with VV polarization.

This paper briefly reviews the technique for generating plane waves using offset parabolas. It also describes the experiment and systems used for data collection. The paper presents results from the experiments.

II. Generation of Plane Wave Illumination

The compact range concept is based on the well-known fact that rays emanating from a spherical source at the focal point of a parabolic reflector are reflected in the form of parallel rays. Any surface normal to this set of parallel rays is an equiphase surface. Thus we can illuminate a surface with a wave having a constant incidence angle, α, as shown in Fig. 1(a).

Because the parabolic reflector is finite, a set of diffracted rays is also generated as shown in Fig. 1(a). Far from the antenna, these diffracted rays are spherical and their amplitude decays as $1/r$. In the immediate vicinity of the reflection boundary (RB), diffracted waves are planar, and they do not decay as a function of range. Fortunately, these rays near the RB propagate at very nearly the same angle as the plane-wave bundle reflected by the parabolic surface. This can be explained by the Uniform Theory of Diffraction (UTD) [12]. In simpler terms it is necessitated by the fact that fields must be continuous across the reflection boundary (Fig. 1);

Manuscript received January 5, 1994.

S. Gogineni and S. Beaven are with the Radar Systems and Remote Sensing Laboratory, University of Kansas, Lawrence, KS 66045 USA.

K. Jezek is with Byrd Polar Research Center, Ohio State University, Columbus, OH 43210 USA.

L. Peters, J. Young, and E. Nassar are with the Electro Science Laboratory, Ohio State University, Columbus, OH 43210 USA.

IEEE Log Number 9411237.

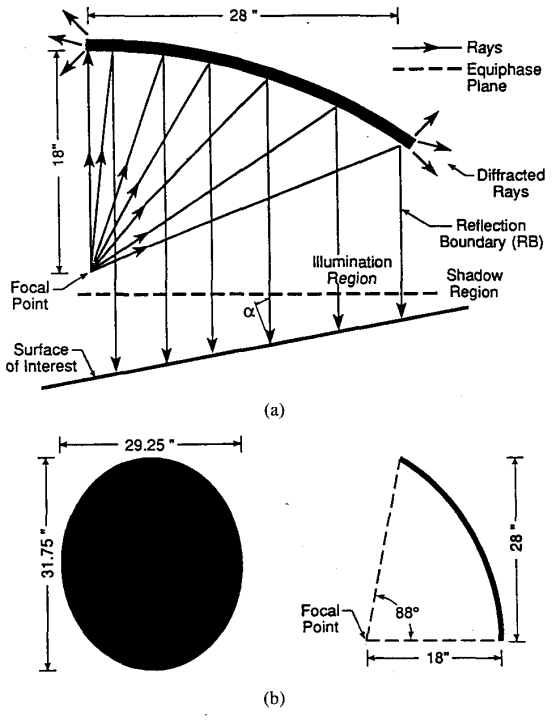

Fig. 1. (a) Offset reflector geometry and (b) physical dimensions of the reflector.

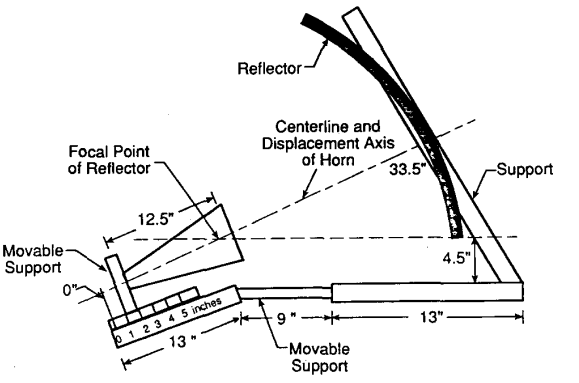

Fig. 2. Physical layout of the plane-wave antenna mount. Support structure for the feed is designed such that the phase center of the feed can be located at the focal point by moving either of the two supports.

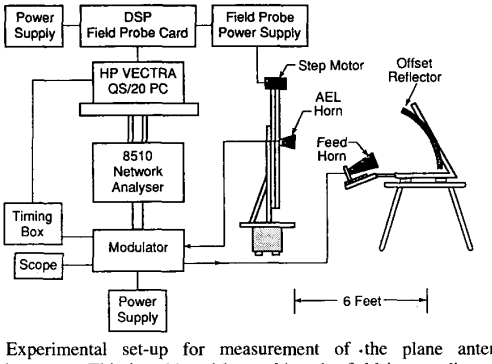

Fig. 3. Experimental set-up for measurement of the plane antenna's near-field patterns. This is achieved by probing the field in two dimensions using a small horn antenna.

i.e., $R^+ + D^+ = D^-$ where R^+ and D^+ represent the reflected and diffracted fields on the illumination side and D^- represents fields in the shadowed region of the reflection boundary. Since R is a plane wave, both D^+ and D^- must also be plane waves near the reflection boundary. A transition function is used to transform the plane-wave fields to the appropriate range-dependent fields. But it is known that the diffracted fields must exhibit range-dependent decay in the region beyond the reflection boundary. The remainder of the diffracted rays represent a source of error. The effect of these can be minimized by edge treatment such as shaping of the edge and/or the use of resistive cards.

The diffracted rays, removed from RB, decay as a function of range, diffraction angle and edge illumination or aperture taper. The use of aperture taper results in a nonuniform plane wave. Unlike a compact range, where it is desirable to generate a uniform plane wave, a nonuniform plane wave is acceptable and even desirable for backscatter measurements over distributed targets. The effect of nonuniformity can be removed during calibration. This can done by measuring the return from the calibration target at several positions within the illuminated spot.

The theory and implementation of the compact antenna range is well documented [10]–[12]. Uniform theory of diffraction and physical optics methods can be used to analyze the problems discussed above. We used mainly an experimental approach for developing the antenna to generate plane waves. We constructed the support structure for the reflector and the feed such that the feed location can be adjusted to place the phase center of the feed at the reflector focal point as shown in Fig. 2. Using a vector network analyzer, we probed the fields from the reflector at the desired distance in two dimensions. We optimized the feed position to obtain plane-wave characteristics at a distance of about 2 meters and at a maximum frequency of operation of 14 GHz. We also measured the field pattern in 2-GHz steps over the entire operating frequency range from 4 to 14 GHz. Fig. 3 shows the experimental set-up used for probing the fields.

Figs. 4 and 5 show measured field patterns at 10 and 12 GHz, respectively. The phase of the field across the illuminated spot of 12 in is constant to within 20° indicating that we indeed simulated a nonuniform plane wave.

III. System Description

To evaluate the utility of the plane-wave antenna for geophysical studies we performed radar measurements with a 10-GHz system. We also made measurements using a 13.5-GHz spherical-wave system to compare its performance with the plane-wave system. Both systems are operated in the step-frequency mode in which the transmitter signal is stepped in frequency over the desired bandwidth, and the amplitude and phase of the received signal are measured at each frequency. We stepped the frequency at 2.5-MHz intervals over

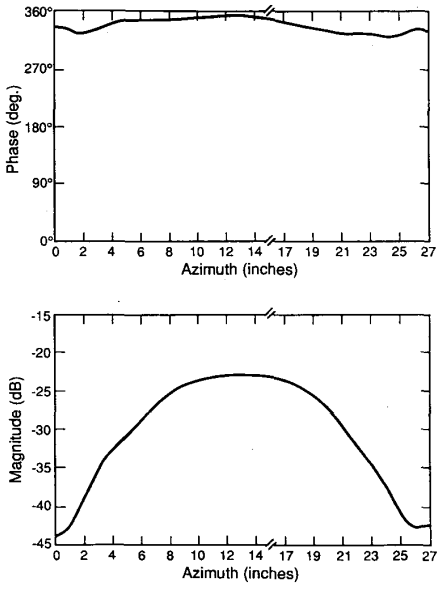

Fig. 4. Near-field horizontal scan for vertical polarization at 2 m from the reflector at 10 GHz. The top figure shows phase as a function of displacement and the bottom figure shows the magnitude of the field. The center of the reflector is located at 13.5 in on these figures.

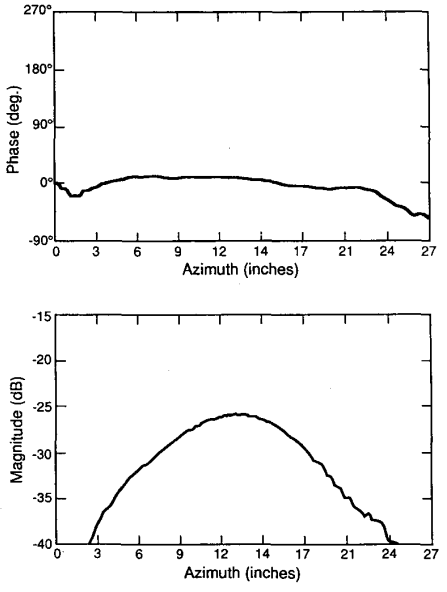

Fig. 5. Near-field horizontal scan for vertical polarization at 2 m from the reflector at 12 GHz. The top figure shows phase as a function of displacement and the bottom figure shows the magnitude of the field. The center of the reflector is located at 13.5 in on these figures.

a 1000-MHz bandwidth. Measured data at all frequencies are concatenated and Fourier-transformed to generate the signal as a function of range or time. This signal is range gated to isolate ice surface return from clutter and is processed to obtain scattering coefficients.

Fig. 6 shows the block diagram of the 10-GHz system. We used a Vector Network Analyzer (VNA) to generate the baseband transmit signal and to measure the amplitude and phase of the received signal. The output from the VNA is upconverted to the desired center frequency using a single sideband upconverter. The amplifier is used to boost the output from the upconverter. The amplifier output is coupled to the antenna through two switches (Switch 1 and Switch 3) and a directional coupler. The directional coupler acts as a duplexer to isolate the receiver from the transmitter. The antenna collects the backscattered signal. This signal passes through the coupled port (4) of the directional coupler and through the switches (Switch 2 and Switch 4) to the mixer. Switch 1 and Switch 2 are used to inject the transmit signal into the receiver for internal calibration. When the system is operated with two dual-polarized antennas, Switch 3 is used to select the desired transmit polarization and Switch 4 is used to select the receive polarization.

TABLE I
KU-BAND STEP-FREQUENCY RADAR SPECIFICATIONS

Table 1. Ku-band Step-Frequency Radar Specifications	
Center Frequency	13.5 GHz
RF Bandwidth	1 GHz
Number of Samples	401
Range Resolution in Air	15 cm
Transmitted Power	10 dBm
IF Frequency	1.7-2.7 GHz
Antennas	*Type:* Diagonal Horn
	Beamwidth: 8.4° (one way)
Polarizations	VV,HH,VH,HV
Calibration	*Internal:* delay line
	External: metal sphere
Data Acquisition	HP8753C Network Analyzer & '386 Personal Computer

The 13.5-GHz system is very similar except for the use of two dual-polarized diagonal horns, one for transmission and the other for reception, and the IF frequency. The use of two antennas eliminates the directional coupler. Table I provides important system parameters including antenna beamwidths for the 13.5-GHz radar.

We calibrated the system by measuring the signal backscattered by a metal sphere of known radar cross section. We estimate absolute calibration uncertainty to be about ±1.5 dB.

IV. EXPERIMENT DESCRIPTION

We performed the radar measurements over simulated sea ice during Apr. 1993. The ice was grown in an outdoor pond of 18 m by 8 m. The pond was equipped with a gantry positioned on rails to facilitate transverse movement to obtain spatially independent samples. We mounted the plane-wave antenna on the gantry such that antenna height above the ice surface was about 2 m. Because of the mounting constraints, the maximum incidence angle for the plane-wave system was restricted to about 35°. We mounted the 13.5-GHz system on the gantry at a height of about 3 m. Incidence angles extended from 0° to 55° for this system. The network analyzer and data acquisition system were housed in a tent adjacent to pond. We used a 50-foot-long RF cable to send VNA output at frequencies between 1 and 3 to the RF section for upconversion. The RF

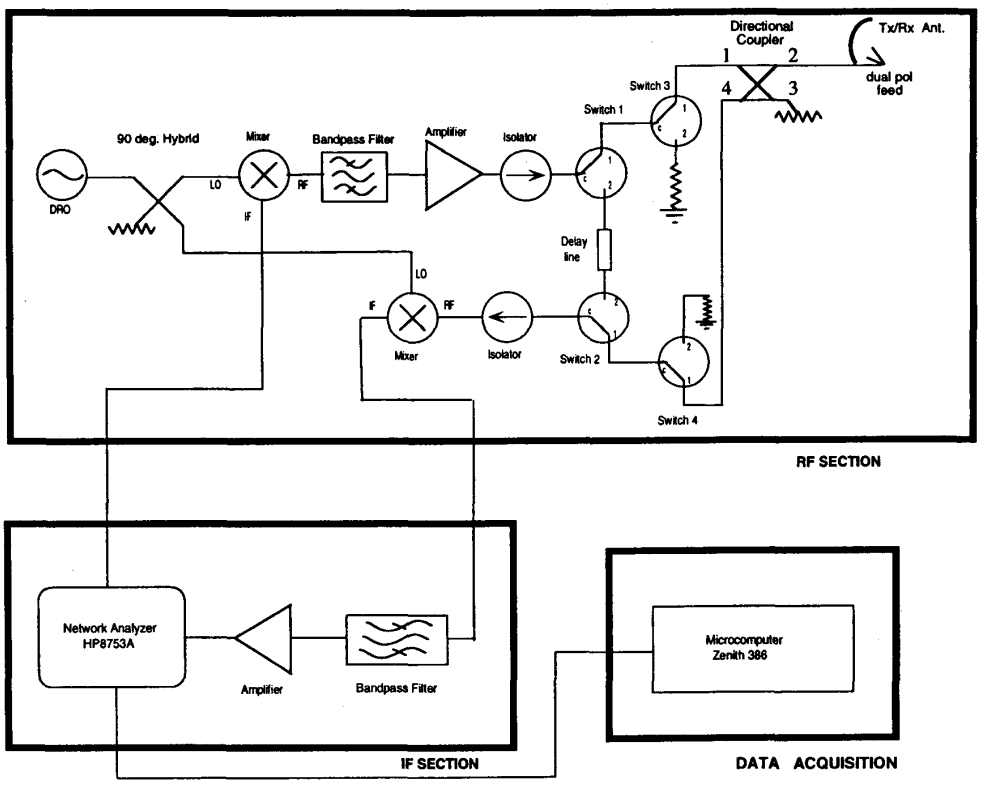

Fig. 6. Block diagram of the X-band radar system. RF section was mounted behind the antenna. IF and data acquisition sections were housed in a tent adjacent to the pond. Two RF cables of about 50-foot length are used to connect RF and IF sections.

section was located behind the antenna. We utilized another 50-foot-long RF cable to send the down-converted signal to the network analyzer for processing. We used systems operating at slightly different frequencies to make nearly simultaneous measurements because we did not have conventional antennas for operation at 10 GHz during this experiment.

We positioned the gantry at the desired location and collected data at 0°, 4°, 10°, 15°, 25°, and 35° using the plane-wave system. We also acquired data over incidence angles from 0° to 55° at 5° intervals with the spherical-wave system. Before starting and after completing measurements at each location, we calibrated both systems internally. We performed similar measurements at three other locations to obtain spatially independent samples.

After completing data collection over the ice we calibrated both radar systems using standard targets of known radar cross section. We used a metal sphere for calibrating the 10-GHz system and a diplane and the metal sphere for calibrating the 13.5-GHz system. In addition to radar measurements, we made measurements of ice surface roughness using a comb gauge. The ice surface was relatively smooth with typical surface roughness of about 2 mm.

V. Results

Because data using the plane-wave antenna were collected in the single antenna mode, these data needed special processing to extract ice returns from feedthrough signals. These feedthrough signals are in general much stronger than target returns. Normally, two approaches are used to reduce these feedthrough signals. First, returns from the background without the target are recorded, and this background return is coherently subtracted from the signal consisting of the background plus target returns. We could not use this approach because we could not point the antenna at the sky because of the maximum incidence angle restriction. Second, some sort of hardware range gate is used to isolate target returns from feedthrough signals. We could not implement this because we did not have access to the very fast switches (switching speed of less than 10 ns) needed. Instead, we used the following method to minimize feedthrough signals.

We assumed that the phase of the return from a distributed target varies randomly from one sample to another whereas the feedthrough signals remain coherent from one sample to another. We coherently averaged four independent samples at each angle. Coherent averaging enhances feedthrough signals, reduces distributed target return substantially and provides an estimate of coherent system noise. We coherently subtracted this average from each sample and Fourier-transformed the subtracted data to determine power received as a function of range. Fig. 7 shows the results at normal incidence before and after coherent subtraction. The scheme we used eliminated the feedthrough signals without significantly affecting the

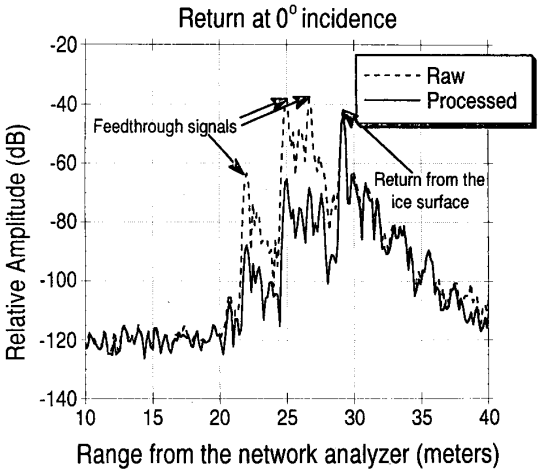

Fig. 7. Radar return as a function of range before and after coherent processing at 0° incidence. Antenna is located approximately 2 m above the ice surface. The first two peaks in the raw data are internal feedthrough signals in the RF section of the radar. The third peak is from the reflection at the antenna feed. Actual range to the ice surface is the difference in distance between antenna feed reflection and ice surface return minus the distance from the feed to reflector surface (≅46 cm).

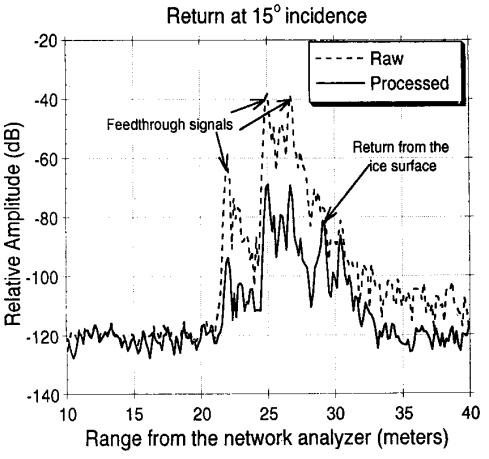

Fig. 8. Radar return as a function of range before and after coherent processing at 15° incidence. Range scale is same as that for Fig. 7.

ice return. This verifies our assumption about coherency of feedthrough signals and random variation of the phase of ice returns from one sample to another. Fig. 8 shows results of measurements at incidence angle of 15° before and after coherent subtraction.

We range-gated the data processed with the procedure described above and computed scattering coefficients using internal and external calibration data.

Fig. 9 compares scattering coefficients determined with plane-wave and spherical-wave systems. These data are the result of averaging four spatial samples. Each spatial sample consists of approximately two independent samples obtained using excess bandwidth [13]. Therefore a minimum of eight independent samples were used in computing the average. This results in an uncertainty of about ±1.6 dB. Scattering

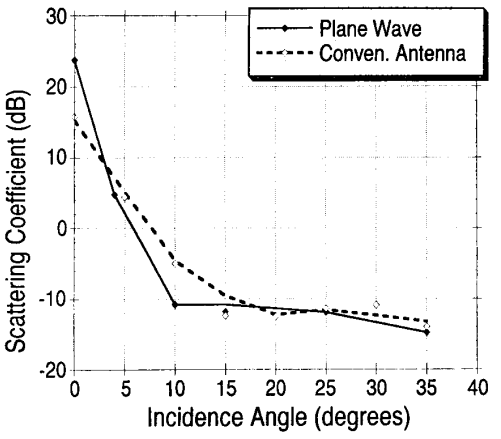

Fig. 9. Comparison of scattering coefficients determined using plane-wave and spherical-wave antennas.

coefficients determined with plane waves decayed by about 35 dB when the incidence angle was increased from 0° to 10°. In contrast, scattering coefficients decreased by only about 20 dB over the same angular region when measured with spherical waves. These results confirm that we can obtain a better estimate of the scattering response near vertical incidence using plane waves generated with offset reflectors operated in the near zone.

VI. Discussion

Near vertical incidence, scattering from a relatively smooth surface consists of two components: 1) a coherent component caused by specular reflection at the dielectric interface; and 2) an incoherent component caused by the rough surface. When the surface is relatively smooth, the coherent component generally dominates the return near vertical. Reference [14] reported a first-order solution to determine the coherent contribution when using finite-beamwidth antennas as

$$\sigma^0_{ppc}\frac{\Gamma_p(\theta)}{B^2}\exp(-4k^2\sigma_h^2)\exp\left(\frac{-\theta^2}{B^2}\right) \tag{1}$$

where p is the polarization, θ is the incidence angle, Γ_p is the power reflection coefficient for polarization p (either H or V), and B is given by

$$B^2 = \frac{1}{(kR_0\beta)^2} + \left(\frac{\beta}{2}\right)^2.$$

The one-sided, 3-dB beamwidth of the antennas is β and the range to the scatterer is R_0.

Using the above equations, the ratio of the coherent component from 10 GHz to 13.5 GHz at normal incidence using antennas with equal beamwidth can be expressed as

$$\frac{\sigma^0_{ppc}(10\text{ GHz})}{\sigma^0_{ppc}(13.5\text{ GHz})}\frac{B^2_{13.5}\exp(-4k_{10}\sigma_h^2)}{B^2_{10}\exp(-4k_{13.5}\sigma_h^2)} \tag{2}$$

where B and k are computed for 10 GHz and 13.5 GHz as indicated by the subscripts.

For an rms surface height of 2 mm this ratio is less than 2 dB at normal incidence.

Reference [15] reported the frequency response of scattering from first-year ice at 40° incidence. These data show that the scattering coefficient increased by about 2 dB from 10 GHz to 13.5 GHz. The theoretical results demonstrate that the scattering characteristics over the angular range between 0° and 40° are nearly similar at 10 and 13.5 GHz. Consequently the difference in scattering response presented in the Results Section (see Fig. 9) can be attributed to the antenna properties.

VII. Conclusion

We used the compact antenna range concept to generate plane waves for measuring the scattering response of distributed targets. To compare the performance of plane-wave and spherical-wave systems in determining the angular response of distributed targets, we performed simultaneous measurements on a relatively smooth saline ice surface. The results show that the plane-wave system provides a better estimate of the near vertical scattering response of distributed targets.

As an extension of this work, we recently developed a 36-inch plane-wave antenna using either a TEM horn antenna operating from 2 to 17 GHz [16] or a bowtie feed horn operating over the frequency range from 500 MHz to 17 GHz [17]. We combined this antenna with a vector network analyzer to develop an ultra wideband radar with a free space range resolution of about 1 cm and angular resolution of about 1°. With this system we have achieved unprecedented control of determining the location and source of scattered energy from a complex material (sea ice). Spatial resolution is achieved by the use of plane wave illumination. Essentially, all portions of a normally incident planar wavefront illuminate the surface simultaneously. This is a major advantage over traditional spherical-wave illumination where targets distributed at different depths but located at identical ranges all appear at the same time. We obtained fine range resolution by the use of wide bandwidth. In addition to the use of the system to identify sources of scattering from various geophysical media, we can also obtain broad spectral electromagnetic signatures of targets.

So far, this approach has been used to study the microwave properties of sea ice. Many other applications can be envisioned. For example, the technique would improve electromagnetic signature data from vegetation by precisely separating signals from leaves, stems and soil. We can also envision applying the technique to forest canopy studies, ocean wave studies, and glacier ice studies.

References

[1] V. H. Anderson, "High altitude, side-looking radar images of sea ice in the Arctic," in *Proc. 4th Symp. Remote Sensing Environ.*, Inst. Sci. Technol., Univ. Michigan, Ann Arbor, 1966, pp. 845–857.

[2] J. W. Rouse, "Arctic ice type identification by radar," *Proc. IEEE*, vol. 57, no. 4, pp. 605–614, 1969.

[3] C. L. Parkinson, J. C. Comiso, H. J. Zwally, D. J. Cavalieri, P. Gloerson, and W. J. Campbell, *Arctic Sea Ice, 1973-1976: Satellite Passive-Microwave Observations*. Washington DC: NASA Scientific and Technical Information Branch, 1987.

[4] F. D. Carsey, Ed., *Microwave Remote Sensing of Sea Ice*. Washington DC: American Geophysical Union, Monograph 68, 1992.

[5] C. E. Livingstone, K. P. Singh, and A. L. Gray, "Seasonal and regional variations of active/passive microwave signatures of sea ice," *IEEE Trans. Geoscience Remote Sensing*, vol. GRS-25, pp. 159–173, Mar. 1987.

[6] M. R. Drinkwater, R. Kwok, D. Winebrenner, and E. Rignot, "Multi-frequency polarimetric SAR observations of sea ice," *J. Geophys. Res.h*, vol. 96, no. C11, pp. 20679–20698, 1991.

[7] D. G. Barber, E. F. Ledrew, D. G. Flett, M. Shokr, and J. Falkingham, "Seasonal and diurnal variations in SAR signatures of sea ice," *IEEE Trans. Geosci. Remote Sensing*, vol. 30, pp. 638–642, May 1992.

[8] R. T. Gedney, R. J. Jirberg, R. J. Schertler, R. A. Mueller, T. L. Chase *et al.*, "All-weather ice information system for Alaskan coastal shipping," in *Proc. 9th Ann. Offshore Technol. Conf.*, Houston, TX, pp. 299–306, 1977.

[9] A. L. Gray, R. O. Ramseier, and W. J. Campbell, "Scatterometer and SLAR results obtained over Arctic sea-ice and their relevance to the problems of Arctic ice reconnaissance," presented at *4th Canadian Symp. Remote Sensing*, Quebec City, PQ, Canada, May, 1977.

[10] C. Pistorius and W. D. Burnside, "An improved main reflector design for compact range application," *IEEE Trans. Antennas Propagat.*, vol. AP-35, pp 342–346, Mar. 1987.

[11] R. G. Kouyoumjian and P. H. Pathak, "A uniform geometrical theory of diffraction for an edge in a perfectly conducting surface," *Proc.IEEE*, vol. 62, pp. 1448–1461, Nov. 1974.

[12] C. E. Ryan, Jr. and L. Peters, Jr., "Evaluation of edge-diffracted fields including equivalent currents for caustic regions," *IEEE Trans. Antennas Propagat.*, vol. AP-17, pp. 292–299, May 1969.

[13] F. T. Ulaby, R. K. Moore, and A. K. Fung, *Microwave Remote Sensing; Active and Passive: Radar Remote Sensing and Surface Scattering and Emission Theory*, Vol. II. Norwood MA: Artech House, 1982.

[14] A. K. Fung and H. J. Eom, "Coherent scattering of a spherical wave from an irregular surface," *IEEE Trans. Antennas Propagat.*, vol. AP-31, pp. 68–72, Jan. 1983.

[15] Y. S. Kim, R. K. Moore, R. G. Onstott, and S. Gogineni, "Toward the identification of optimum radar parameters for sea-ice monitoring," *J. Glaciology*, vol. 31, no. 109, pp. 214–219, 1985.

[16] K. Jezek, P. Gogineni, L. Peters, J. Young, S. Beaven *et al.*, "Microwave scattering from saline ice using plane wave illumination," *IGARRS '94 Dig.*, pp. 493–495, 1994.

[17] A. K. Y. Lai, A. L. Sinopoli, and W. D. Burnside, "A novel antenna for ultra-wide-band applications," *IEEE Trans. Antennas Propagat.*, vol. 40, pp. 755–760, July 1992.

Sivaprasad Gogineni received the Ph.D. degree from the University of Kansas, Lawrence.

He is currently a Professor in the Department of Electrical Engineering and Computer Science at the University of Kansas and Director of the Radar Systems and Remote Sensing Laboratory. He has been involved in research on the application of radars to the remote sensing of sea ice, ocean, and land. He has authored or coauthored more than 30 journal publications and many technical reports and conference presentations. He was actively involved in developing instrumentation for radar systems currently being used at the University of Kansas for backscatter measurements. He has also participated in field experiments in the Arctic and on towers in the open ocean.

Dr. Gogineni is a member of URSI Commission F and the Electromagnetics Academy. In 1991, he was awarded the Miller Award for Engineering Research from the University of Kansas and the Taylor and Francis 1991 Best Letter Award.

K. C. Jezek, received the Ph.D. degree from the University of Wisconsin, Madison.

He is Director of the Byrd Polar Research Center and Associate Professor in the Department of Geological Sciences at Ohio State University, Columbus. His present research interests include continental-scale observations of Earth's ice cover using spaceborne remote sensing techniques. He has been particularly involved in projects to acquire, process and analyze ERS-1 and JERS-1 synthetic aperture radar data collected over the Arctic and Antarctica. Most recently, he has been involved in planning for the complete radar mapping of Antarctica with Radarsat.

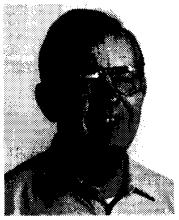

Leon Peters, Jr. (S'50–A'51–SM'60–F'81–LF'89) was born May 28, 1923, in Columbus, OH. He received the B.E.E., M.Sc., and Ph.D. degree from Ohio State University, Columbus, in 1950, 1954, and 1959, respectively.

In 1950, he became a Research Associate in the ElectroScience Laboratory, Department of Electrical Engineering, Ohio State University, where he is now the Director. In 1960, he joined the teaching staff at Ohio State University, where he is now a Professor Emeritus in the Department of Electrical Engineering. He has served as Technical Area Director for electromagnetic and remote sensing and as the Associate Department Chairman for Research. His research interests are in the fields of antennas, microwaves, and properties of radar targets.

Dr. Peters is a member of Sigma Xi and Commission B of the International Union of Radio Science.

Jonathan D. Young, (S'61–M'82) received the B.E.E., M.Sc., and Ph.D. degrees from Ohio State University, Columbus, in 1964, 1965, and 1971, respectively.

He has been with the ElectroScience Laboratory, Ohio State University, since 1971. He has been engaged in research on radar target scattering signatures and imaging, ultra-wideband radar antennas, measurements, and scattering analysis, and Ground Penetrating Radar studies. Since 1983, he has been serving as the Associate Director of the ElectroScience Laboratory. From 1991 to 1994, he served on the Ohio State University Research Committee. His recent studies on radar target scattering diagnostics have concentrated on measurements and analysis of scattering phenomenology at frequencies below 2 GHz, where foliage penetrating radars operate. He holds four patents on the Terrascan, a radar buried utility locator system for detecting plastic as well as metal pipes. His recent studies have concentrated on systems which can combine target identification with detection for buried targets. Some of his most recent research involves the application of radar sensing to Automated Highway system needs.

Dr. Young is a member of Tau Beta Pi, Eta Kappa Nu, and Sigma Xi. He held offices in the local IEEE AP-S Chapter from 1984 to 1986, when the chapter won two outstanding chapter awards. He won an IR100 Award from *Industrial Research Magazine* in 1978.

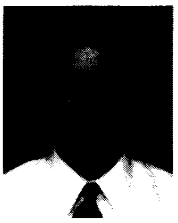

Scott G. Beaven received the B.S. and M.S. degrees in electrical engineering from the University of Kansas, Lawrence, in 1990 and 1992, respectively. He is currently pursuing the Ph.D. degree at the same university.

He has worked as a Research Assistant and Teaching Assistant at the University of Kansas. His research interests include microwave remote sensing of sea ice, *in situ* backscatter measurements and SAR image analysis.

Mr. Beaven is a member of Eta Kappa Nu, Tau Beta Pi, Sigma Pi Sigma, and ASEE. He was awarded an Office of Naval Research doctoral fellowship in 1990.

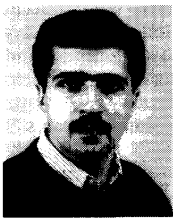

E. M. Nassar was born in Lebanon in August 1967. He received the B.S. degree in electrical engineering from American University, Beirut, Lebanon, and the M.S.E.E. degree in electrical engineering from Ohio State University, Columbus, in 1990 and 1992, respectively. He is pursuing the Ph.D. at the latter university.

Since 1990, he has been working as a Graduate Research Assistant at the ElectroScience Laboratory, Ohio State University. His research interests include electromagnetic scattering, computational electromagnetics, microwave remote sensing, and broad band antennas.